

# Supporting information

## Impact of fluorinated end groups on the properties of acceptor-donor-acceptor type oligothiophene for solution-processed photovoltaic cells

Guangrui He,<sup>1</sup> Xiangjian Wan,<sup>1</sup> Zhi Li,<sup>1</sup> Qian Zhang,<sup>1</sup> Guankui Long,<sup>1</sup> Yongsheng Liu,<sup>1</sup> Yanhui Hou,<sup>2</sup> Mingtao Zhang,<sup>3</sup> Yongsheng Chen<sup>1,\*</sup>

### Part 1 Figures and Tables

Figure S1. Maldi-FTMS of DCAE7T-F1 -----	2
Figure S2. Maldi-FTMS of DCAO7T-F7-----	2
Figure S3. XRD of DCAE7T-F1+PC <sub>61</sub> BM-----	3
Figure S4a. <sup>1</sup> HNMR of DCAO7T-F7-----	3
Figure S4b. <sup>19</sup> FNMR of DCAO7T-F7-----	4
Figure S4c. <sup>13</sup> CNMR of DCAO7T-F7-----	4
Figure S5a. <sup>1</sup> HNMR and <sup>13</sup> CNMR of DCAE7T-F1-----	5
Figure S5b. <sup>19</sup> FNMR of DCAE7T-F1-----	5
Figure S5c. <sup>13</sup> CNMR of DCAE7T-F1-----	6
Figure S6. J <sup>0.5</sup> vs V plots for the pure DCAE7T-F1 film at room temperature.-----	6
Figure S7. Contact angle of the DCAO7T-F7 solution in CHCl <sub>3</sub> dropped onto an ITO surface.--	6
Figure S8. SM BHJ devices based on a blend of DCAE7T-F1/PC <sub>61</sub> BM (1/0.5) with different position in ITO substrate-----	7
Figure S9. EQE spectra of optimized SM BHJ device of DCAE7T-F1 : PC <sub>61</sub> BM (2:1)-----	7
Table S1. XRD data of DCAE7T-F1, DCAO7T-F7, DCAE7T and DCAO7T-----	8
Table S2. SM BHJ devices based on DCAE7T-F1 at different positions of ITO substrate.-----	8
Table S3. XPS data of DCAE7T-F1:PC <sub>61</sub> BM at different positions of ITO substrate.-----	8
Part 2 Some discussion and introduction	
I. Something about spin coating-----	9
II. The purity check of these donors in the organic solar cells-----	9
III. The detailed calculation process of the surface energy-----	10
References-----	11

## Part 1 Figures and Tables

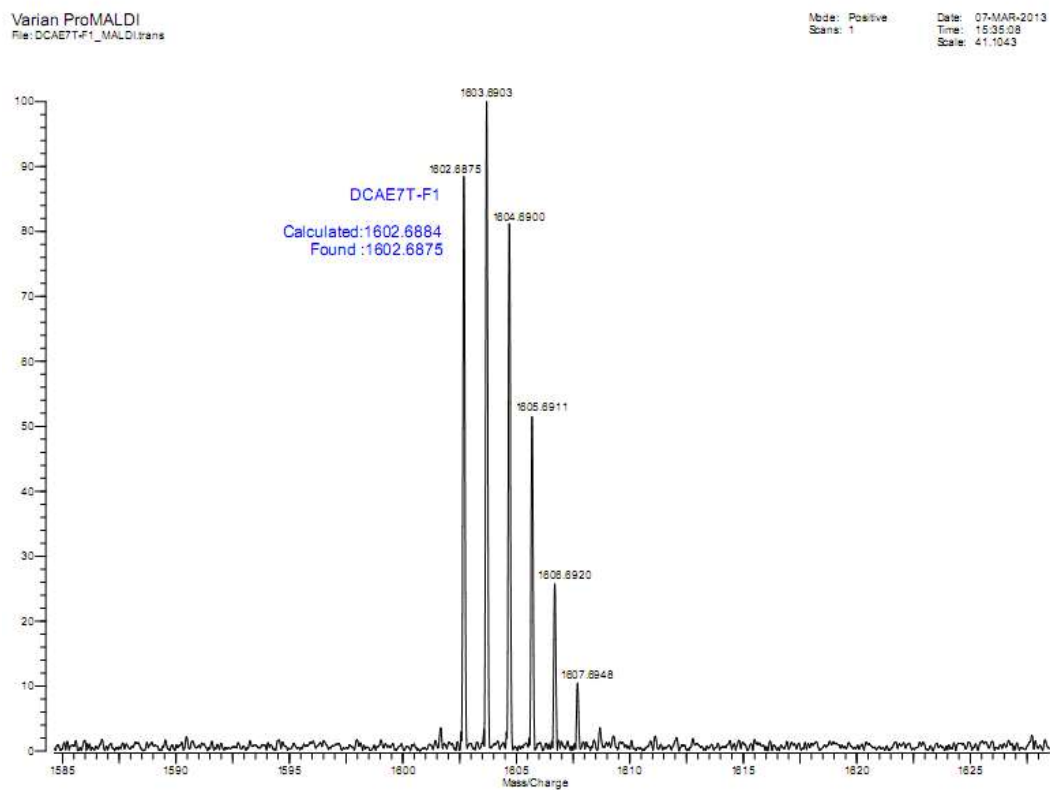


Figure S1. Maldi-FTMS of DCAE7T-F1

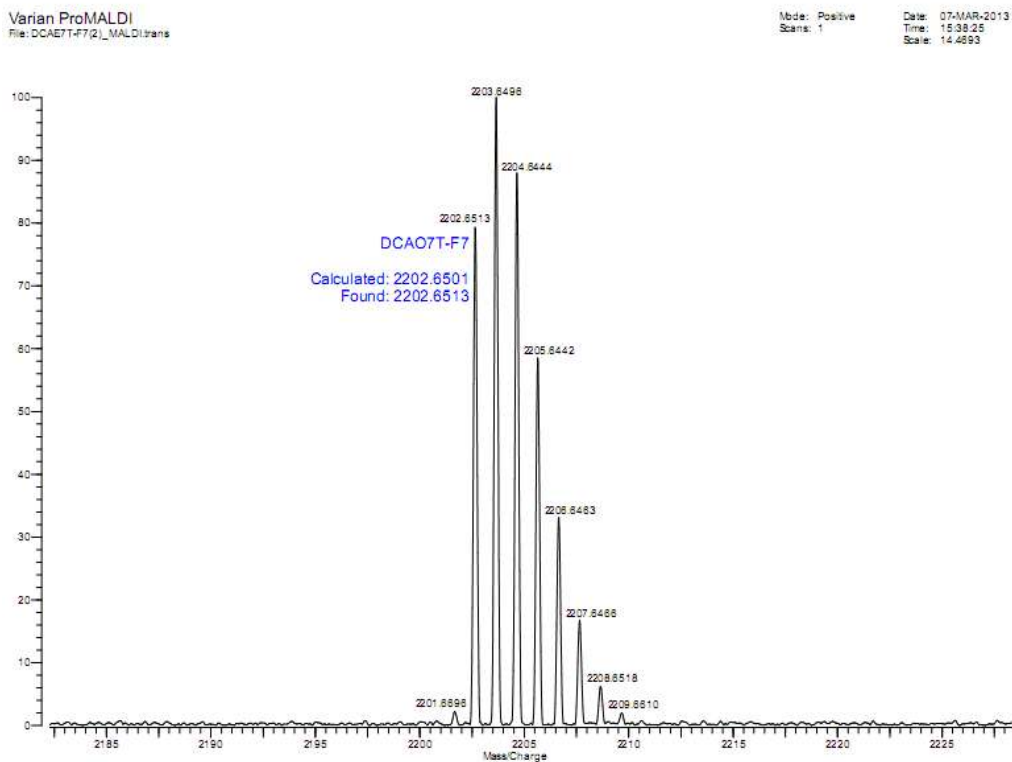


Figure S2. Maldi-FTMS of DCAO7T-F7

Figure

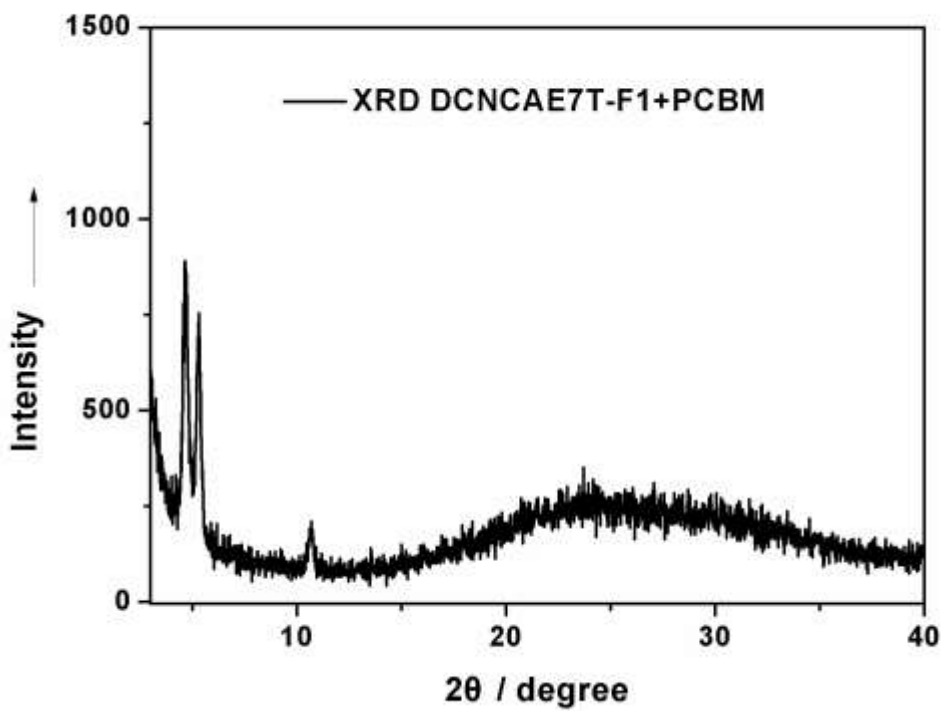


Figure S3. XRD of DCAE7T-F1+PC<sub>61</sub>BM

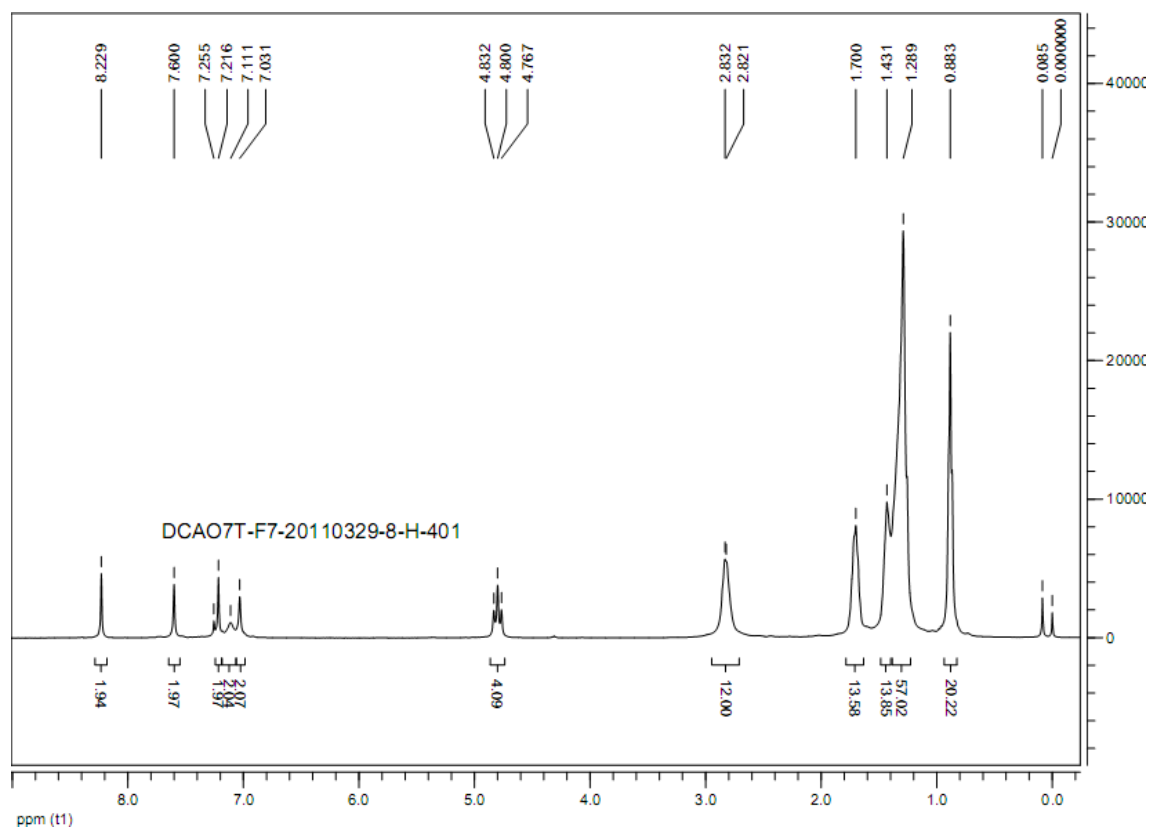


Figure S4a. <sup>1</sup>H NMR of DCAO7T-F7

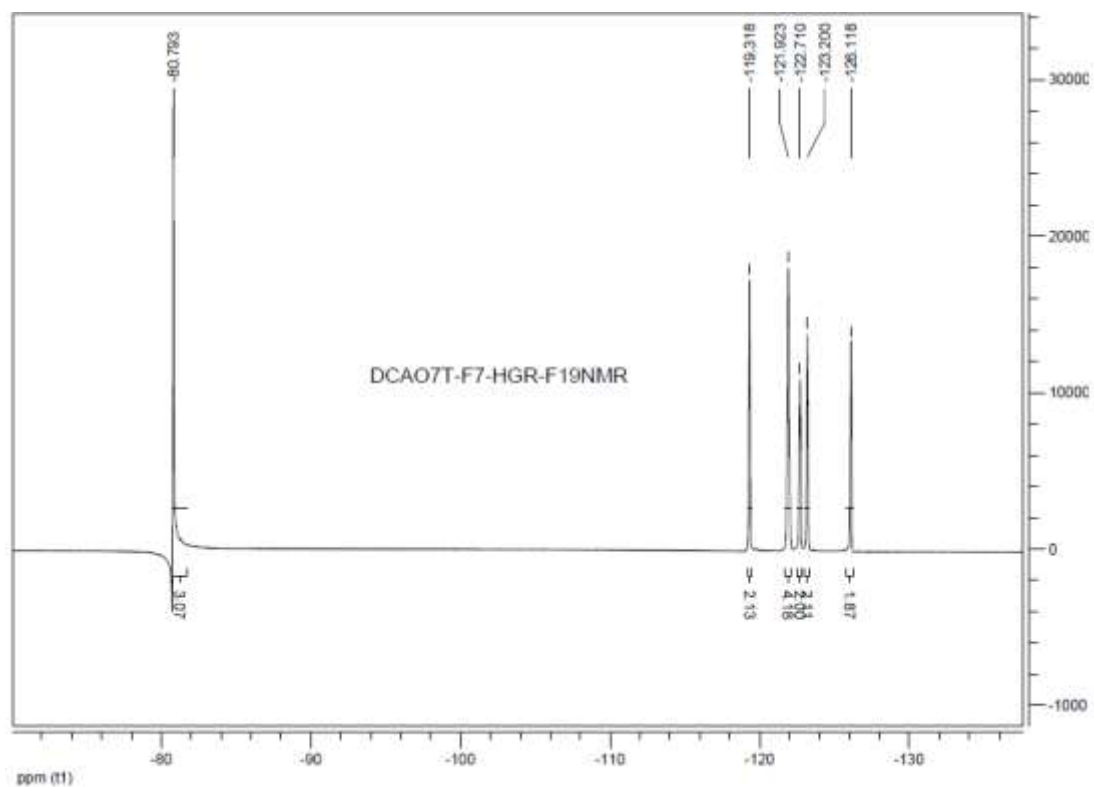


Figure S4b. <sup>19</sup>F NMR of DCAO7T-F7

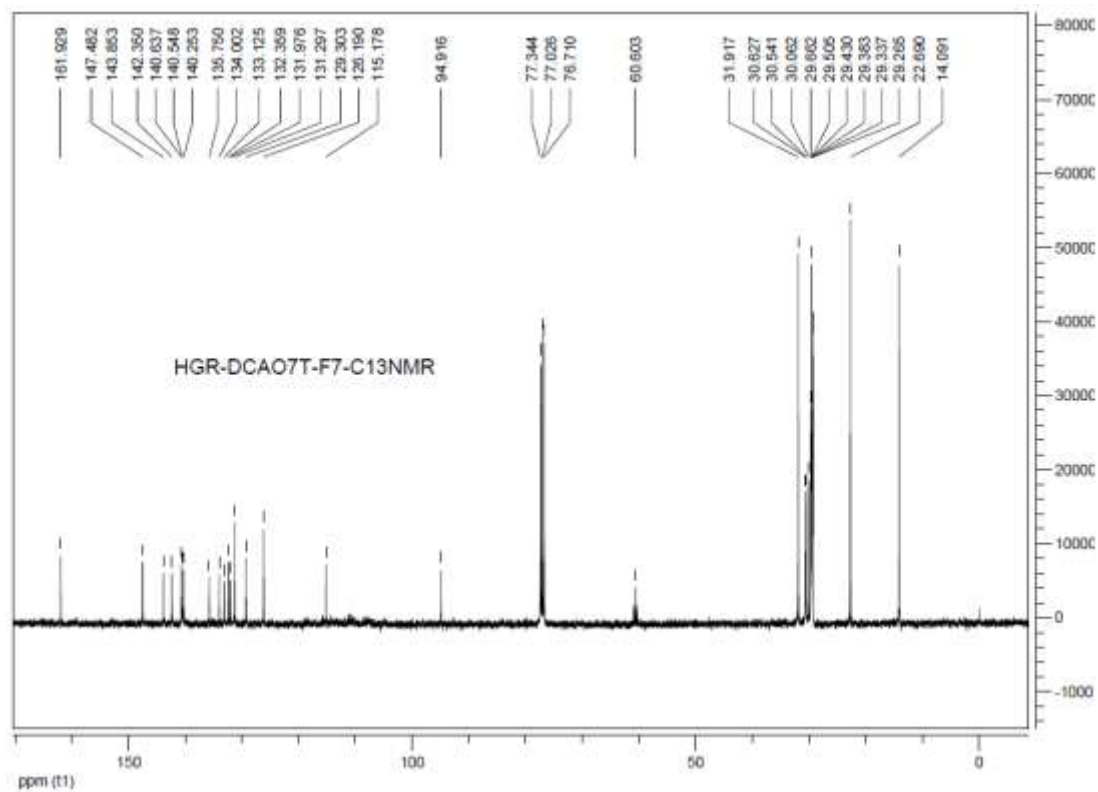


Figure S4c. <sup>13</sup>C NMR of DCAO7T-F7

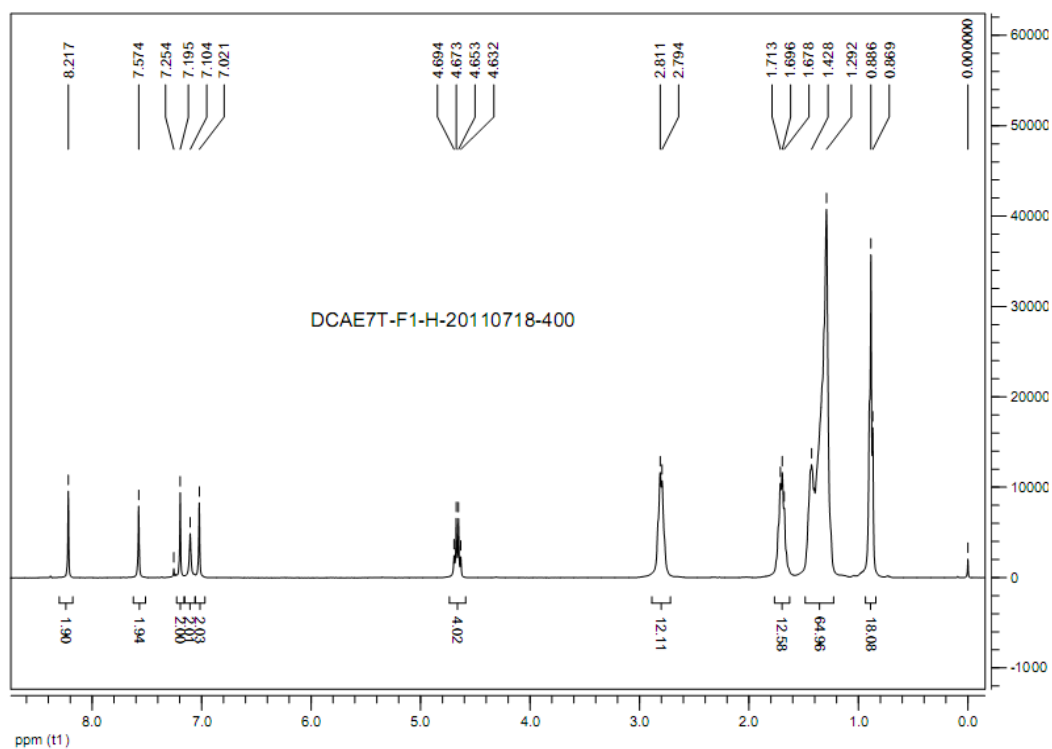


Figure S5a.  $^1\text{H}$ NMR of DCAE7T-F1

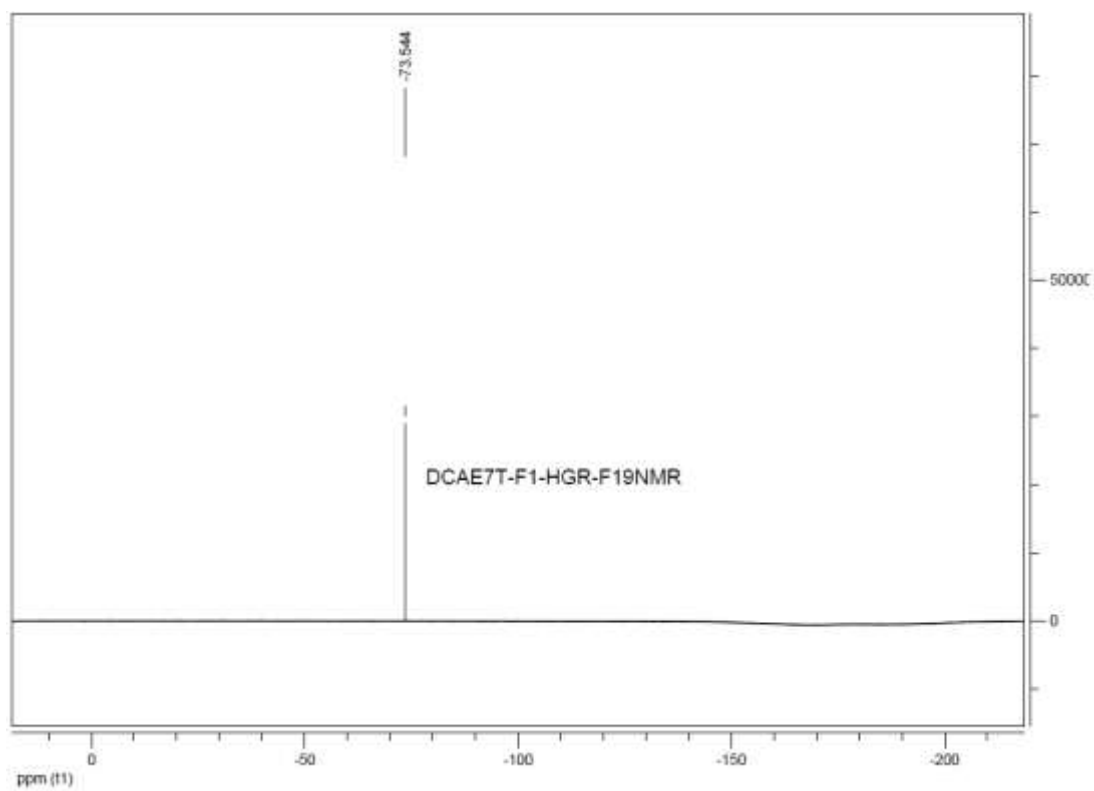


Figure S5b.  $^{19}\text{F}$ NMR of DCAE7T-F1

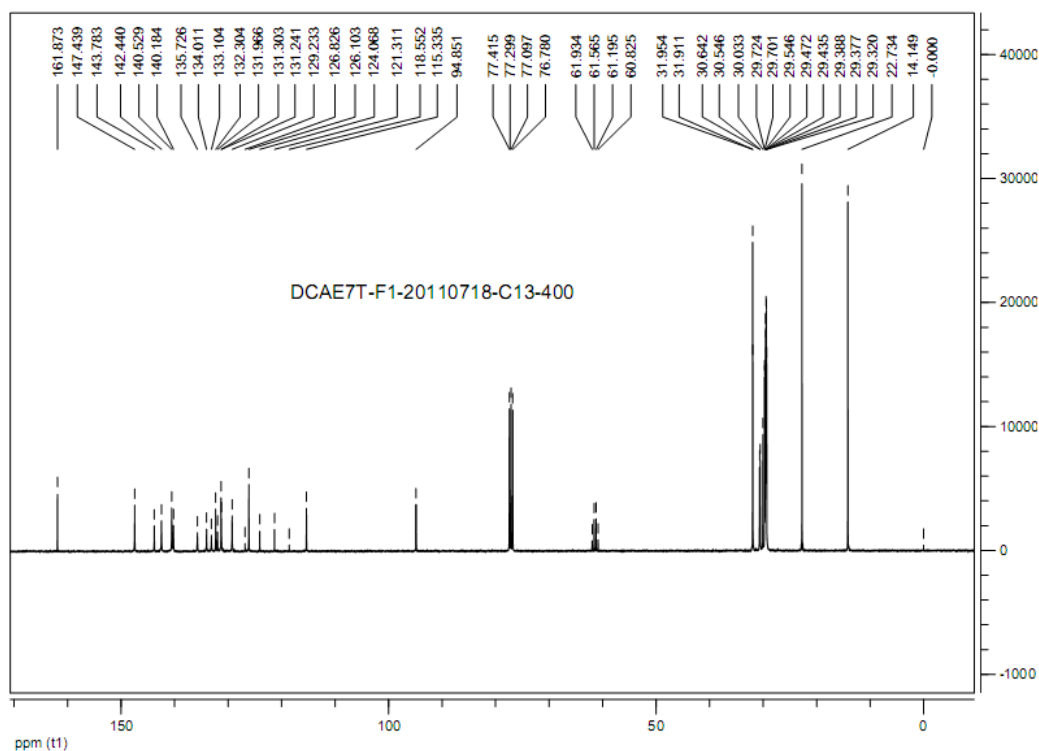


Figure S5c.  $^{13}\text{C}$ NMR of DCAE7T-F1

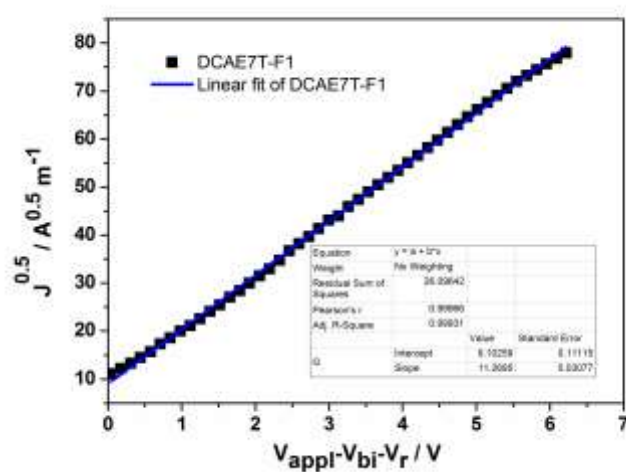


Figure S6.  $J^{0.5}$  vs  $V$  plot for the pure DCAE7T-F1 film at room temperature.



Figure S7. Contact angle of DCAE7T-F7 solution in  $\text{CHCl}_3$  dropped on the ITO surface.

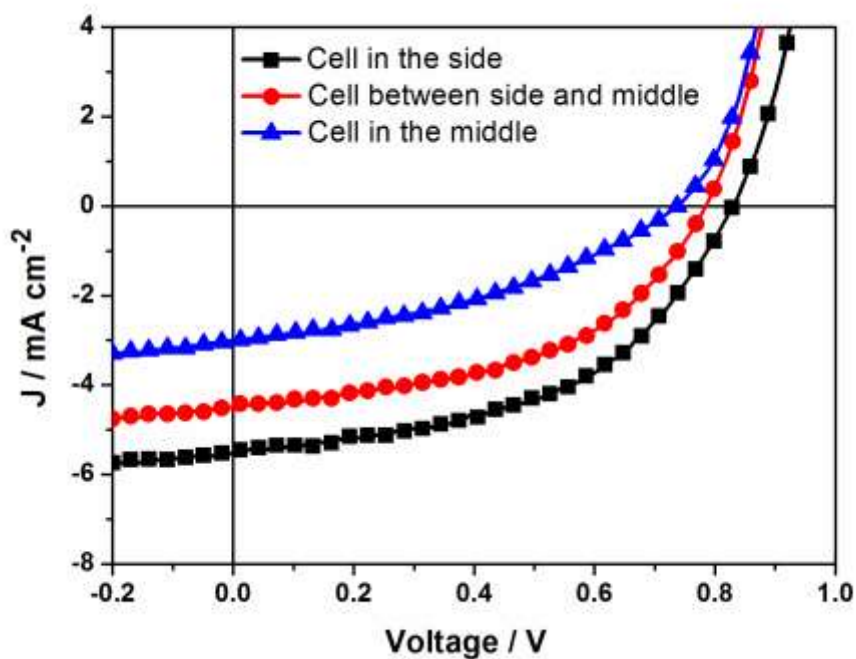


Figure S8. Current density-voltage characteristics of the SM BHJ devices based on the blend of DCAE7T-F1/PC<sub>61</sub>BM (1/0.5) with different positions on the ITO substrate under an illumination of AM.1.5, 100 mW/cm<sup>2</sup>.

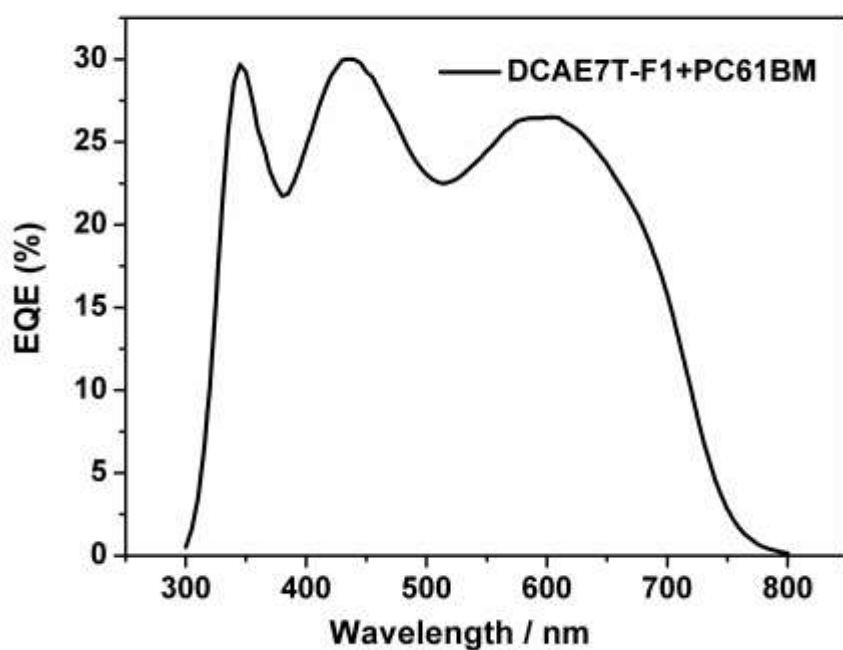


Figure S9. EQE spectra of optimized SM BHJ device of DCAE7T-F1 : PC<sub>61</sub>BM (2:1).

**Table S1. XRD data of DCAE7T-F1, DCAO7T-F7, DCAE7T and DCAO7T**

<b>Compounds</b>	<b>XRD Peaks 2θ-(intensity)</b>	<b>(100) 2θ-(intensity)</b>	<b>(200) 2θ-(intensity)</b>	<b>(300) 2θ-(intensity)</b>
DCAE7T-F1		5.36-(6840)	10.72-(1246)	16.16-(326)
DCAO7T-F7		4.04-(3193)	8.08-(926)	12.19-(781)
DCAE7T		4.76-(31756)	9.54-(2097)	14.38-(708)
DCAO7T <sup>a</sup>		4.22-(43744)	8.57-(2014)	12.85-(1076)

**Table S2. Summary of SM BHJ devices based on DCAE7T-F1 at different positions of ITO substrate.**

<b>Place in the ITO</b>	<b>V<sub>oc</sub> / V</b>	<b>J<sub>sc</sub> / mA cm<sup>-2</sup></b>	<b>FF (%)</b>	<b>PCE (%)</b>
Edge	0.83	5.50	0.50	2.26
Between Edge and Middle	0.78	4.53	0.49	1.73
Middle	0.74	3.03	0.38	0.85

**Table S3. XPS data of active layer DCAE7T-F1:PC<sub>61</sub>BM (2:1) at different position of ITO substrate.**

<b>Place in the ITO</b>	<b>C Mass Conc %</b>	<b>S Mass Conc %</b>	<b>F Mass Conc %</b>
Edge	80.92	9.99	9.09
Middle	80.07	10.63	9.30
Calculated	70.46	11.50	5.84



## Part 2 Some discussion and introduction

### I. Something about spin coating<sup>1</sup>

1. The pioneering analysis of spin coating was performed by Emil et al fifty years ago<sup>2</sup>
2. A centrifugal force drives the liquid radially outward. The viscous force and surface tension causes a thin residual film to be retained on the flat substrate.
3. Spin coating can be broken down into four key stages : (1). Dispense the fluid; (2). spin; (3). stable fluid out flow; (4). evaporation
4. Several processing parameters involved in the spinning process are : dispense method, volume of fluid, final spin speed ( $w$ ), final film thickness, solution viscosity, solution concentration ( $c$ ), spin time, *etc.*
5. For stages (1) and (2), wettability of the substrate by the polymer solution, more importantly the solvent, as a dilute solution is generally used for spin coating, which is important for the spreading of the dispensed drop and finally the uniform film formation with the aid of centripetal forces.<sup>3</sup>
6. For stages (3) and (4), the viscous flow effect dominates early on while the evaporation process dominates later.
7. Evaporation of solvent leads to a rapid increase in the viscosity of the polymer film (vis-a-vis reduction in the mobility of the polymer molecules), thereby leading to deposition of the film.

### II. The purity check of these donors in the organic solar cells

The purity of small molecule donors plays an important role in determining the final performance of small molecule solar cells.<sup>4</sup> Sometimes the small amounts of the impurity can destroy the organic device.

We have check the purity of these four small molecules using <sup>1</sup>HNMR, <sup>19</sup>F NMR, <sup>13</sup>CNMR, TLC and MS (Maldi).

1. Firstly, the product was subjected to chromatography on silica gel using a mixture of dichloromethane and petroleum ether. From TLC, we condensed the pure part of the product.
2. Second, from NMR especially the <sup>1</sup>HNMR, we can see the purity degree of these donors. MS can support the HNMR result.
3. Third, before OPV device fabrication, the donor small molecule was dissolved in chloroform, and methanol was added. The precipitate was collected. The procedure was repeated several times until no impurity dot can be found in the condensed filtrate on the TLC.

### III. The detailed calculation process of the surface energy

The surface free energy of these films was calculated using the van Oss treatment (Lifshitz and electron donor–electron acceptor components of surface free energy)<sup>5,6</sup>

van Oss et al. assumed that the surface free energy ( $\gamma$ ) may be decomposed into two components, the Lifshitz–van der Waals component ( $\gamma^{\text{LW}}$ ) and the acid–base component ( $\gamma^{\text{AB}}$ ):

$$\gamma = \gamma^{\text{LW}} + \gamma^{\text{AB}} \quad (1)$$

the acid–base term can be divided into two components,  $\gamma^+$  (an electron-acceptor term) and  $\gamma^-$  (an electron-donor term), which are complementary in nature and together yield the acid–base component,  $\gamma^{\text{AB}}$ :

$$\gamma^{\text{AB}} = 2(\gamma^+ \times \gamma^-)^{1/2} \quad (2)$$

The surface free energy of a solid may then be described by three components and the complete Young–Dupre equation becomes:

$$\gamma_{\text{L}}(1 + \cos \theta) = 2 \cdot \sqrt{\gamma_{\text{S}}^{\text{LW}} \cdot \gamma_{\text{L}}^{\text{LW}}} + 2 \cdot \sqrt{\gamma_{\text{S}}^+ \cdot \gamma_{\text{L}}^-} + 2 \cdot \sqrt{\gamma_{\text{S}}^- \cdot \gamma_{\text{L}}^+} \quad (3)$$

The three components of the surface free energy of the solid,  $\gamma_{\text{S}}^{\text{LW}}$ ,  $\gamma_{\text{S}}^-$  and  $\gamma_{\text{S}}^+$  may then be calculated from contact angle measurements of three testing liquids (water, diiodomethane and ethylene glycol) with known values of the surface tension components.<sup>6</sup>

#### Surface Tension Components and Parameters of Liquids, Measured at 20°C

Test liquid	$\gamma_{\text{L}}$ (mJ/m <sup>2</sup> )	$\gamma_{\text{L}}^{\text{LW}}$ (mJ/m <sup>2</sup> )	$\gamma_{\text{L}}^+$ (mJ/m <sup>2</sup> )	$\gamma_{\text{L}}^-$ (mJ/m <sup>2</sup> )
Water	72.8	21.8	25.5	25.5
Diiodomethane	50.8	50.8	0.0	0.0
Ethylene glycol	48.0	29.0	1.92	47.0

Then the the surface free energy of the solid  $\gamma_{\text{S}}$  can be obtained.

$$\gamma_{\text{S}} = \gamma_{\text{S}}^{\text{LW}} + 2(\gamma_{\text{S}}^- \times \gamma_{\text{S}}^+)^{1/2} \quad (4)$$

## References

- 1 N. Sahu, B. Parija, S. Panigrahi, *Indian Journal of Physics* **2009**, *83*, 493-502.
- 2 A. G. Emslie, F. T. Bonner, L. G. Peck, *Journal of Applied Physics* **1958**, *29*, 858-862.
- 3 S. Roy, K. J. Ansari, S. S. K. Jampa, P. Vutukuri, R. Mukherjee, *ACS Applied Materials & Interfaces* **2012**, *4*, 1887-1896.
- 4 W. L. Leong, G. C. Welch, L. G. Kaake, C. J. Takacs, Y. Sun, G. C. Bazan, A. J. Heeger, *Chemical Science* **2012**, *3*, 2103-2109.
- 5 C. J. Van Oss, M. K. Chaudhury, R. J. Good, *Chemical Reviews* **1988**, *88*, 927-941.
- 6 M. H. V. C. Adão, B. J. V. Saramago, A. C. Fernandes, *Journal of Colloid and Interface Science* **1999**, *217*, 94-106.